LATTICE DESIGN FOR THE ILSF BOOSTER SYNCHROTRON

E. AHMADI, F. SAEIDI, Iranian Light Source Facility, IPM, Tehran, Iran
H. GHASEM, School of Particles and Accelerators, IPM, Tehran, Iran

Abstract

The Iranian Light Source Facility (ILSF) booster synchrotron is a full energy injector of 3 GeV ILSF storage ring. The lattice concept based on separate tunnel layout and the main features of the optics are described. The closed orbit correction scheme, evolution of beam parameters during ramping and effect of eddy current on the dynamic aperture will be discussed.

INTRODUCTION

A full energy 3 Gev booster synchrotron has been designed for ILSF project to boost 150 MeV electron beam, extracted from Linac, to the target energy of 3 GeV The main feature of the booster is small emittance and hence small size of the aperture and compact magnetic elements. After considering different symmetries and circumferences for geometry of the booster, ultimately a four-fold symmetry lattice was selected for the booster [1]. We have used the traditional approach in housing booster relative to storage ring and the booster will be mounted in different tunnel from the storage ring's tunnel. To keep low the construction cost, the same shielding walls has been planned to accommodate service area in between the booster and storage ring. The circumference of the designed booster is 192 m and the average distance between booster and storage ring is about 17 m. Natura beam emittance in the booster is 32.42 nm.rad and its main parameters are listed in Table 1 [2].

LATTICE LAYOUT

The booster consists of four super periods in which each super period contains 5 theoretical Minimum emittance (TME) cells and two matching cells. The TME cells consists of 1.1908 m combined function bending magnet with embedded defocusing sextupole componen and focusing combined function quadrupole magnet with embedded focusing sextupole component. The embedded sextupole fields in the bending and focusing quadrupole magnets are used for correcting natural chromaticity and optimizing dynamic aperture. The matching cell consists of a bending magnet the same as the bending magnet o unit cells, two focusing quadrupoles with embedded sextupole field and three separate function defocusing quadrupoles. Two individual sextupole magnets has been placed in the matching cell to correct chromaticity induced by eddy currents in the vacuum chamber o bending magnets. The optical functions in one super period are shown in figure 1.

Table 1: Main parameters of the booster synchrotron

Parameter	Unit	Value
Energy	GeV	3
Circumference	m	192
Number of super periods	-	4
Horizontal emittance	nm.rad	32.42
RF frequency	MHz	500
Natural energy spread	-	8.74×10^{-4}
Tune (Q_x/Q_y)	-	11.22/4.29
Natural chromaticity (ξ_x/ξ_y)	-	-19.87/-10.01
Momentum compaction (α_c)	-	5.90×10^{-3}
Rep. rate	Hz	2

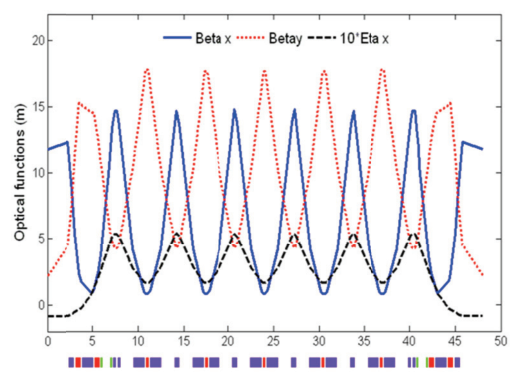

Figure 1: The optical functions in one super period of the booster.

CLOSED ORBIT CORRECTION

The magnet misalignment and field errors produce closed orbit distortion (COD), which should be corrected to small values. Orbit correction system of the booster synchrotron consists of 32 beam position monitors, 32 horizontal and 28 vertical correctors. Distribution and number of the correctors are chosen in a way to provide good closed orbit correction with reasonable value of corrector's strength.

To examine orbit correction scheme, a computer simulation of COD has been carried out by BETA [3]. A set of COD samples were calculated with random misalignments and field errors applied to each magnet. The utilized errors are presented in Table 2.

ISBN 978-3-95450-122-9

Table 2: Misalignment and Field Errors in the Magnets

Type of error	**Value**
Dipole displacement	Δx=Δy=150 μm
Quadrupole displacement	Δx=Δy=150 μm
sextupole displacement	Δx=Δy=150 μm
Magnet rolling errors	Δφ=100 μrad
Dipole field error	0.01%

The orbit correction system of the booster synchrotron consists of 36 beam position monitors (BPM), 36 horizontal correctors (HC) and 28 vertical correctors (VC). The location of BPMs, HC and VC along the phase advance of electrons in one supper period of the booster is shown in figure 2. We have summarized the results of closed orbit correction in the Table 3.

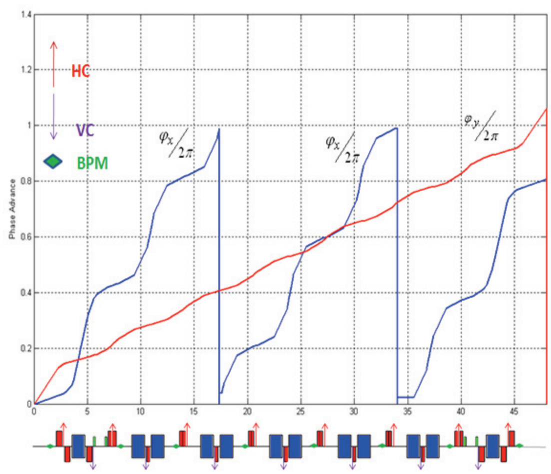

Figure 2: Position of horizontal (HC), vertical (VC) correctors and beam position monitors (BPM) in booster.

Table 3: Closed Orbit Correction Results

	Before correction	
	horizontal	**vertical**
Maximum orbit distortion around ring (mm)	15.2	13.9
Average orbit distortion around ring (mm)	2.82	2.61
	After correction	
Residual orbit around ring (mm)	1.16	1.10
Average corrector strength (mrad)	0.0885	0.115

TIME EVLUTION OF BEAM PARAMETERS

Beam parameters like emittance and energy spread will change during acceleration. Time evolution of emittance in the booster is given by [4, 5]

$$\frac{d\varepsilon}{dt} = -\frac{1}{\gamma(t)}\frac{d\gamma(t)}{dt}\varepsilon - \frac{2}{\tau_x}\varepsilon + \frac{1}{J_x}\frac{2}{\tau_x}C_q\gamma^2(t)\frac{I_5}{I_2} \quad (1)$$

where J_x, τ_x and $\gamma(t)$ are horizontal damping partition number, horizontal damping time and relativistic Lorentz factor respectively. Figure 3 shows the evolution of emittance during ramping.

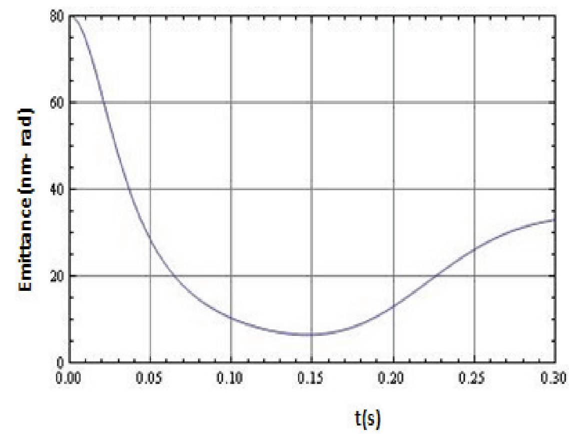

Figure 3: Time evolution of the beam emittance during ramping.

Time evolution of energy spread square is given by [4, 5]

$$\left.\frac{d\sigma^2}{dt}\right|_{eq.} = C_q\gamma^2(t)\frac{2}{J_z\tau_z}\frac{I_3}{I_2} - \left(\frac{2}{\tau_z} + \frac{1}{\gamma(t)}\frac{d\gamma(t)}{dt}\right)\sigma^2 \quad (2)$$

Where J_z, τ_z are longitudinal damping partition number and longitudinal damping time respectively. Figure 4 shows the evolution of energy spread during ramping.

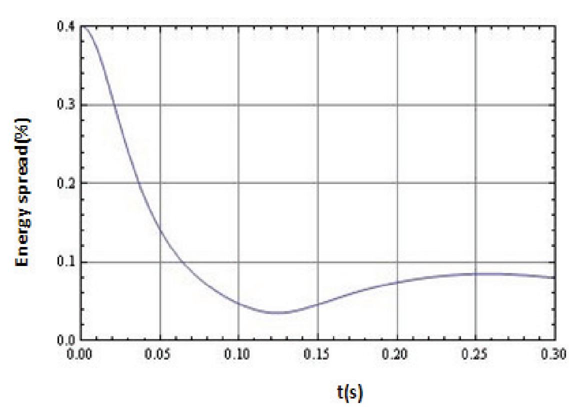

Figure 4: Time evolution of energy spread during ramping process.

EDDY CURRENT EFFECTS

Time varying fields in booster dipole magnets induce eddy current and result multipole components in the dipole vacuum chambers. The most important multipole produced by eddy current is the sextupole component which changes the natural chromaticity of the booster. The general equation which describes the induced sextupole field by eddy currents is given by [5, 6]

$$\mathrm{m}=\frac{1}{2B\rho}\frac{\partial^2 B}{\partial x^2}$$

$$\mathrm{m}=\frac{\mu_0 \delta e}{h\rho}\frac{2\pi f}{\alpha-\cos 2\pi ft}\sin 2\pi ft \, J\left(\frac{b}{a}\right) \tag{3}$$

For the ILSF booster, half horizontal radius a is 23 mm and half vertical radius of vacuum chamber b is 8.8 mm and the width of vacuum chamber e is 1 mm and the function J is calculated to 0.6 (see Ref. [4, 5]). In the ILSF booster, the embedded sextupole components in bending and focusing quadrupole magnets have been used for correcting the natural chromaticity and optimizing the dynamic. However, the induced sextupole components will change the sextupole strength lead to change the chromaticity during the ramping process. By using two separate families of focusing and defocusing sextupoles, we have fixed the chromaticity during ramping. The dynamic aperture of on energy electrons with and without eddy current is depicted in figure 5. The dynamic aperture tracking has been done for the worst case when the energy of electrons is 325 MeV. As seen, eddy current lead to shrinkage of dynamic aperture but this is still adequately larger than the physical aperture.

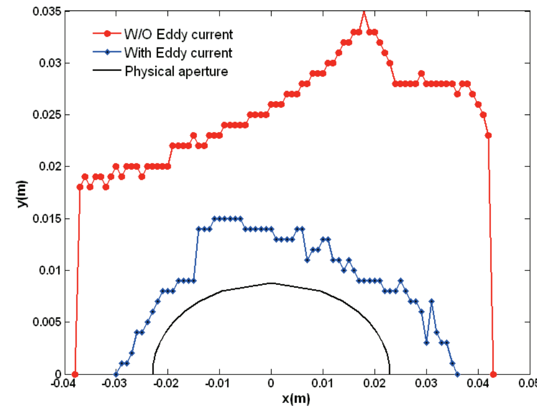

Figure 5: Dynamic aperture of booster with and without eddy current, (ξ_x=ξ_y=+1).

ACKNOWLEDGMENTS

The authors would like to sincerely thank professor Dieter Einfeld and Professor Helmut Wiedemann for their continuous scientific support to the ILSF project.

REFERENCES

[1] Beam dynamic groups, internal report, (2011).
[2] H. Ghasem et al., Booster design for ILSF, Proceedings of IPAC 2011.
[3] L. Farvacque, T.F. Guenzel, J.L. Laclare, ESRF, Grenoble, third edition, July 2001.
[4] Andy Wolski, *Low-emittance machines*, CAS, Daresbury, UK, September 2007.
[5] Taiwan Photon Source (TPS) conceptual design report, June 2008.
[6] F. Iazzourene, “Updated lattice for the ELETTRA Booster synchrotron”, ST/M-00/2 April 2001.

ISBN 978-3-95450-122-9